

UNCERTAINTY AND WING STRUCTURAL WEIGHT APPROXIMATIONS

Melih Papila* (papila@aero.ufl.edu)

Raphael T. Haftka† (haftka@ufl.edu)

Department of Aerospace Engineering,
Mechanics & Engineering Science,
University of Florida
Gainesville, FL 32611-6250

Abstract

The paper explores the effect of numerical noise and uncertainties on response surface approximations for wing bending material weight for a high speed civil transport (HSCT) design. The accuracy of the response surface approximations is improved by identification and repair of outliers present in the data due to noisy structural optimization. The use of correction response surface approximations is also investigated. Error analysis compares the importance of noise and modeling error sources in approximation. The most accurate approximation is studied for sensitivity to uncertainty in problem data. The data are treated as fuzzy variables and the vertex method is applied to calculate the uncertainty in wing bending material. Substantial variation in levels of uncertainty is found over the design space.

Introduction

In preliminary design of aircraft, structural weight equations based on analytical predictions and historical data are often used (see in Torenbeek¹). They may not be, however, accurate enough for new aircraft concepts since the historical data may not fit well new concepts. The high speed civil transport (HSCT) aircraft and uninhabited combat aerial vehicle (UCAV), for example, are new classes of aircraft for which historical data is sparse.

Accuracy of available weight equations for new aircraft concepts can be checked, and equations can be modified or customized through the use of multiple structural optimizations and response surface (RS) approximations. Balabanov et al.² developed quadratic polynomial response surfaces for wing bending material weight of HSCT aircraft as functions of 29 configuration design variables. Their study showed that response surfaces can improve on traditional weight equations available in the flight optimization system (FLOPS), but not by much. The fact that the improvement was modest was surprising since the response surface approximation was tailored to an HSCT with narrow range of geometric configurations and weights.

For improved response surface approximations, analysis of potential sources of error, outliers in data and the inadequacy of quadratic polynomials (modeling error), is an important issue. One of the main advantages of using response surface approximation is the inherent filtering of noise in data (e.g. Giunta et al.³). Numerical noise generated in the structural optimization procedure based on finite element analysis might be substantial and create so called outliers. Modeling error might also contribute to the accuracy of approximation in an adverse manner if the weight is not modeled well by quadratic polynomials. Therefore identifying and eliminating outliers and reducing the modeling error can improve substantially the accuracy of the response surface approximations.

In the design process of a new concept like HSCT, modifications and changes in geometry are likely. For example, a new airfoil more efficient aerodynamically, but with slightly different thickness to chord ratio might be developed. Similarly, advances in material technology might produce a new material with slightly different density, but increased yield stress.

* Graduate Research Assistant

† Professor, Fellow AIAA

Therefore it is important to determine how sensitive is the design to such changes. Response surface approximations make design against uncertainty computationally affordable because they allow for an inexpensive evaluation of the effect of such changes (e.g. Venter and Haftka⁴). Venter and Haftka⁵ employed a fuzzy set model of uncertainty, and used the vertex method (Dong and Shah⁶) for calculating the possibility of failure in dropped ply composite laminate design. In this study all configuration variables are treated as uncertain parameters or fuzzy variables as well as material properties, density and yield stress, and the effect of the uncertainty of parameters on wing bending material is studied.

The objectives of the present paper are to investigate how to obtain more accurate weight equations by response surface approximations and to find their sensitivity to uncertainty in material properties and geometry. A number of structural optimizations based on finite element analysis are performed to generate bending material weight in configuration design space for five HSCT configuration variables. Response surface approximations are constructed for wing bending material weight. Iteratively re-weighted least square method (IRLS), stepwise regression and a detailed error analysis are employed in order to improve the approximations. Finally, response surface approximation, fuzzy set theory and the vertex method are used for comparing designs in terms of their sensitivity to uncertainty.

Response Surface Approximations

Response surface methodology is a popular multi-point approximation tool (Myers and Montgomery⁷). The method approximates the numerical or physical experimental data by an analytical expression which is usually a polynomial called response surface. It assumes that the response surface expression is exact, and the differences, called residuals, between the experimental data and the surface function are due to normally distributed noise in the experiments. The response surface estimate at a design point j described with the vector \mathbf{x}_j , is obtained by linear regression with coefficient estimates b_i and assumed shape functions \mathbf{x}_i , usually monomials, as

$$\hat{y}_j = \sum_{i=1}^{n_b} b_i \mathbf{x}_i(\mathbf{x}_j) \quad (1)$$

The error or residual between the exact and the estimate defined in Eq. 1 for the same point is expressed as

$$e_j = y(\mathbf{x}_j) - \hat{y}_j \quad (2)$$

The residual can now be written in a matrix form for n_d data points,

$$\mathbf{e} = \mathbf{y} - \mathbf{X}\mathbf{b} \quad (3)$$

where \mathbf{X} is the matrix whose component (i, j) is the shape function, $\mathbf{x}_j(\mathbf{x}_i)$. The coefficient vector \mathbf{b} in Eq. 3 is solved for residual vector $\mathbf{e} = 0$ in a least-square sense, and the remaining error vector, \mathbf{e}_r is found to satisfy

$$\mathbf{e}_r^T \mathbf{e}_r = \mathbf{y}^T \mathbf{y} - \mathbf{b}^T \mathbf{X}^T \mathbf{y} \quad (4)$$

An unbiased estimate of the root-mean-square (rms) error, $\hat{\mathbf{S}}$ is given as

$$\hat{\mathbf{S}} = \sqrt{\frac{\mathbf{e}_r^T \mathbf{e}_r}{n_d - n_b}} \quad (5)$$

The Estimated Standard Error, e_{es} called also prediction variance, is a direct measure of the error in the response surface estimate at a design point. It is expressed as,

$$e_{es} = \hat{\mathbf{S}} \sqrt{(\mathbf{x}^m)^T (\mathbf{X}^T \mathbf{X})^{-1} (\mathbf{x}^m)} \quad (6)$$

where \mathbf{x}^m is the vectors of shape functions, $\mathbf{x}_j(\mathbf{x}_i)$ used in Eq. 1 calculated at the point where the response is to be predicted. The predictive power of the approximation may be measured by the quantity R_a^2

$$R_a^2 = 1 - \frac{\mathbf{e}_r^T \mathbf{e}_r / (n_d - n_b)}{\sum_{i=1}^{n_d} (y_i - \bar{y})^2 / (n_d - 1)} \quad (7)$$

where \bar{y} is the average value of the response. An R_a^2 value larger than 0.9 is typically required for an adequate approximation

Fuzzy Set Theory

Fuzzy set theory was introduced by Zadeh⁸ as a mathematical tool for quantitative modeling of uncertainty. In contrast to classical set theory where an element either completely belongs to a specific set or not at all, fuzzy set theory makes use of membership

functions to denote the degree to which an element belongs to the fuzzy set under consideration. The membership function of a fuzzy set \mathbf{A} , assigns a grade of membership, ranging between 0 and 1, to each element of the universal set, \mathbf{Z} , and can be represented alternatively as

$$\mathbf{m}_A(z) : \mathbf{Z} \rightarrow [0,1] \quad (9.a)$$

$$\mathbf{A}(z) : \mathbf{Z} \rightarrow [0,1] \quad (9.b)$$

The double use of the same symbol, \mathbf{A} , in Eq. (9.b) for membership function besides fuzzy set itself does not result ambiguity since each fuzzy set is completely and uniquely defined by only one particular membership function. In this paper Eq. (9.a) is used to denote membership functions.

Fuzzy sets may be represented numerically by making use of \mathbf{a} level cuts. An \mathbf{a} level cut is defined as the real interval where the membership function is larger than a given value, \mathbf{a} (Klir and Yuan⁹, p. 19) and may be written mathematically for a generic fuzzy set \mathbf{A} as follows:

$${}^a A = \{z \mid \mathbf{m}_A(z) \geq \mathbf{a}\} \quad (10)$$

Equation 10 is shown graphically in Fig. 1.a, where it is assumed that \mathbf{A} has a triangular membership function. Also shown in Figure 1.a are the end points, ${}^a a_1$ and ${}^a a_2$ of the considered \mathbf{a} level cut.

A fuzzy number is defined as a fuzzy set that is both normal and convex (Klir and Yuan⁹, p. 97). A normal fuzzy set has a maximum membership function value equal to 1, while all possible \mathbf{a} level cuts are convex for a convex fuzzy. The fuzzy set \mathbf{A} with membership function \mathbf{m}_A shown in Fig. 1.a is thus a fuzzy number. In fact the triangular and symmetric membership function is most often used to represent fuzzy numbers, mainly due to its simplicity. As shown in Fig. 1.a, any triangular fuzzy number may be represented by only three variables: $z_L; z_N$ and z_U .

A fuzzy function \mathbf{Y} is a function of fuzzy variables \mathbf{Z}_i and may be written as

$$\mathbf{Y} = \mathbf{f}(\mathbf{Z}_1, \mathbf{Z}_2, \dots, \mathbf{Z}_n) \quad (11)$$

for the case where n fuzzy variables are considered. When all the fuzzy variables of a fuzzy function are continuous fuzzy numbers, the fuzzy function itself is also a continuous fuzzy number (Klir and Yuan⁹) and its membership function as schematically represented in Fig. 1.b, can be obtained by the vertex method (Dong and Shah⁶).

HSCT Design Problem

The problem studied in this paper is a 250 passenger HSCT design with a 5500 n.mi. range and cruise Mach speed of 2.4. A general HSCT model^{10,11,12} developed by the Multidisciplinary Analysis and Design (MAD) Center for Advanced Vehicles at Virginia Tech includes 29 configuration design variables. Of these, 26 describe the geometry, two the mission, and one the thrust, see Table 1. Load cases for HSCT design studies are given in Table 2, where the first two reflect normal flight conditions, and the others represent severe and critical limit cases. A simplified version of the problem with four geometric variables defining wing shape, and fuel weight, W_{fuel} among the original 29 is used here, following Knill et al¹². The four geometric configuration variables are root chord, c_{root} , tip chord, c_{tip} , in-board leading edge (LE) sweep angle L_{LE} , and the thickness to chord ratio for the airfoil, t/c . Figure 2 shows a typical wing planform of the HSCT and the configuration variables used here. These five variables were configuration variables throughout the first part of this study, while fuselage, vertical tail, mission and thrust related parameters are kept unchanged.

Structural Optimization

In this study, a structural optimization procedure based on finite element analysis using the GENESIS program¹³ was applied. A finite element model developed by Balabanov^{2,10,11} was used. The model, shown in Fig. 3, uses forty design variables, including 26 to define skin panel thicknesses, 12 for spar cap areas, and two for the rib cap areas. The objective function is the total wing structural weight. The structural optimization is performed for N aircraft configurations, and the flowchart of the calculations is shown in Fig. 4. The HSCT codes^{10,11,12} calculate aerodynamic loads for the load cases given in Table 2. A mesh generator by Balabanov² creates the finite element mesh, distributes the aerodynamic and inertia loads onto the structural nodal points and generates input for GENESIS.

Response Surface Construction

The HSCT configuration variables, cv_i have different order of magnitudes, and so they normalized, to the range $(-1, +1)$ as

$$x_i = \frac{cv_i - [\max(cv_i) + \min(cv_i)]/2}{[\max(cv_i) - \min(cv_i)]/2} \quad (12)$$

First a central composite design (CCD) was used to select 43 configurations representing the design space. JMP¹⁴ was used to fit a quadratic polynomial to the results of 43 structural optimizations. Mixed mode (both backward and forward elimination) stepwise regression was used to eliminate poorly characterized coefficients of the quadratic polynomial. Next, an analysis of the effect of the different variables was carried out. Based on the significant terms having high t-statistic values in the quadratic approximation, 6 cubic terms were selected. Additional 27 configurations were optimized to allow us to characterize these terms together with quadratic terms and construct a cubic approximation. To see the effect of increasing the number of design points, a quadratic response surface based on all 70 design points was also constructed. The first four rows of Table 3 summarize the results using the root mean square error predictor (RMSE) as a measure of accuracy and the R_a^2 as a measure of the reliability of the fit. From Table 3 it is seen that increasing the number of design points improved the approximation more than that achieved by adding cubic terms selected based on significant terms.

Outlier analysis

The results obtained for wing bending material weight calculations through structural optimization by GENESIS for a given configuration could differ by up to 30% depending on the optimization method, move limits and computer used. Table 4 gives examples for the differences in the optimization results.

This observation was considered an indication of numerical noise which could cause outliers (points with excessive errors) and could adversely affect the accuracy of the response surface. In order to check the existence of outliers and identify them, IRLS (Iteratively Reweighted Least Square) method in JMP was used. The method is an iterative fitting procedure, using weights for points with large residuals, and the weighting formula is given as

$$weight = \begin{cases} \left[1 - \left(\frac{|r/s|^2}{B} \right) \right]^2 & \text{if } |r/s| \leq B \\ 0 & \text{otherwise} \end{cases} \quad (13)$$

where r : residual (response data minus fitted response)
 s : estimate of standard deviation or rms error
 B : A tuning constant, usually $1 < B < 3$ (here 1.9 and 2.5)

Of the basic 43 configurations of the CCD, four configurations were identified as outliers by IRLS with weights smaller than 0.01. These four designs were re-optimized by using several different initial values of structural design variables, and by changing the choice of optimization method in GENESIS. The re-optimization procedure resulted in lower WBMW for three out of four candidate outlier configurations. Then, a new response surface approximation was constructed from the updated or repaired data. In order to show how the process affects the approximation fit to the structural optimization results, the optimum WBMW vs. the corresponding approximations are given in Fig. 5. Figures 5-a, b and c show the IRLS approximation with marked outliers, RS constructed from original 43 data, and RS based on repaired 43 data, respectively.

Modeling Error analysis

Besides noise and outliers, there is modeling error because the true weight is not a quadratic function of the design variables. In this study, approximation with more cubic terms is also studied to evaluate the modeling error. To be able to characterize and find the cubic coefficients, additional design points are necessary. Therefore, another set of 43 design points were obtained by the face centered CCD with lower and upper limits of -0.75 and 0.75, respectively, so that this new design box is inside the original design box with a common center point. Together with the previous seventy points, the new points give a total of 112 design points. IRLS and re-optimization were also applied to check for outliers and to repair the detected ones, respectively. Then, this set of 112 design points was used in the construction of the response surface. Two approximations, quadratic and cubic, are constructed. The cubic model was obtained after mixed mode stepwise regression procedure. Their estimated RMS errors are also given in Table 3. With the repair procedure for outliers and cubic reduced model, the error was reduced by half, with about half of the improvement coming from the repair procedure.

Design Line Study

In order to estimate how much of the error is due to numerical noise and how much due to modeling error, a design line (alpha line) study was performed. The design line in this study is the line connecting the vertex of lower limits to the vertex of upper limits, where all design variables are all -1 and all +1, respectively. A schematic representation of this extreme value design line is shown in Fig. 6-a for a three-dimensional design box. Along the extreme value design line for the 5 configuration variables, twenty one

equally spaced points were used as shown in Fig. 6-b. Structural optimization results were obtained at these 21 points, and points that peaked markedly over the trend were repaired by re-optimization.

With 21 points along a one-dimensional line, we assumed that a cubic fit to the 21 points is more exact than the structural optimization values because it eliminates most of the noise. This 1-D cubic fit is considered here as the “truth” model.

Finally, the truth model for design line was compared with the quadratic and cubic response surface approximations obtained over the whole design space. Figure 7 shows repaired Genesis results, the 1-D truth model, and the response surface approximation predictions along extreme value design line. From the figure it is clear that substantial error due to noise remains. Figure 8 shows the error analysis including estimated standard errors e_{es} for both RS approximations and their absolute errors based on the cubic truth model. It can be concluded that noise and modeling errors are of similar magnitude. The modeling error appears to cancel the error due to noise in the left half of the line. Table 3 also presents the summary for RS approximations over the whole design space.

Correction Response surface

Reducing modeling error by using cubic polynomials greatly increases the number of required structural optimizations. In order to avoid this step, the response surface was used to correct an available wing bending material weight equation instead of fitting the data directly. The equation is taken from Flight Optimization Systems (FLOPS) which is a multidisciplinary system of computer programs for conceptual and preliminary design and evaluation of advanced aircraft concepts (McCullers¹⁵). The correction was done by fitting a response surface to the ratio, \bar{w} , of the GENESIS predicted weight, $W_{BMW_{GEN}}$, and the FLOPS predicted weight, W_{FLOPS}

$$\bar{w} = \frac{W_{BMW_{GEN}}}{W_{BMW_{FLOPS}}} \quad (14)$$

The wing bending material weight by correction response surface, $W_{BMW_{CRS}}$, is then obtained by multiplying the approximated ratios, \bar{w}_{RS} , by W_{FLOPS} , as

$$W_{BMW_{CRS}} = \bar{w}_{RS} W_{FLOPS} \quad (15)$$

The advantage of a correction response surface over a standard response surface depends on the goodness of the simple model which is used in the correction. The FLOPS weight equation has proved in the past to correlate well with GENESIS optimization. Consequently the correction factor \bar{w} varies over a small range and can be modeled well by a quadratic polynomial.

Table 5 summarizes results obtained with the correction response surface. It can be easily seen that the errors using the correction are substantially smaller than the corresponding values in Table 3 except for the last row. With the correction response surface it is possible to obtain with 43 corrected points and a quadratic model error level that required 112 corrected points and the cubic models without correction. It appears that the correction response surface reduces the modeling error so that the cubic terms are no longer needed. However, repair is still needed to reduce the noise error. Since the repaired data is already available, a design line study and error analysis are also performed for correction response surface. Figures 9 and 10 present the truth-approximation comparison and error analysis, respectively, for correction response surfaces on the alpha line.

Sensitivity to Uncertainty

RS approximations are useful for investigating the sensitivity to uncertainty of design using fuzzy set methods (Venter and Haftka⁵). In the present paper, the effect of uncertainties in geometry and material properties were studied.

The reduced cubic response surface approximation, for wing bending material weight, RS_{cubic} is treated as the fuzzy function in this study. The approximation, in fact, was constructed as function of five configuration variables while keeping the density and yield stress at nominal titanium values. These material parameters, fortunately, may easily be related with structural weight when stress constraints dominate. When only stress constraints are present, it is clear that structural weight is proportional to density and inversely proportional to yield stress of the material used. Buckling and minimum gage constraints complicate the relationship. Here, the relation between the structural weights for two different materials is assumed as

$$\frac{(W_s)_2}{(W_s)_1} = \bar{b}f_r + \mathbf{g} \quad (16)$$

$$\text{where } \bar{f}_r = \frac{(\mathbf{r}/\mathbf{s}_y)_2}{(\mathbf{r}/\mathbf{s}_y)_1} \quad (17)$$

With only stress constraints, the constants \mathbf{b} and \mathbf{g} are equal to 1 and 0, respectively. In order to determine these constants, six of the configurations with different levels of bending material weight and with different number of active minimum gage constraints were studied. The best fit to the data was

$$\mathbf{b} = 0.7612$$

$$\mathbf{g} = 0.2388$$

The uncertain wing bending material weight problem, \mathbf{W}_b , as our fuzzy function can now be expressed as function of the seven uncertain variables: root chord length, tip chord length, leading edge sweep angle, thickness to chord ratio, fuel weight (configuration variables), density and yield stress (material related variables) $x_1, x_2, x_3, x_4, x_5, ?$ and s_y , respectively.

$$\mathbf{W}_b = (0.7612 \frac{?/s_y}{(\mathbf{r}/\mathbf{s}_y)_{nominal}} + 0.2388) \mathbf{RS}_{cubic} \quad (18)$$

$$\mathbf{RS}_{cubic} = f(x_1, x_2, x_3, x_4, x_5)$$

Triangular membership functions are assumed for all fuzzy variables. The fuzzy variables, their ranges, and their uncertainty levels are summarized in Table 6. The membership function of the response, wing bending material weight, is determined through the vertex method. The magnitude of the uncertainty in weight associated with the uncertainty in the input values in Table 6 is illustrated along a design line connecting the lower bound and upper bound point. Figure 11 shows the nominal values as well as the lower and upper bounds on the membership function of the weight. From Fig. 11 it can be seen that the assumed uncertainty in the variables may cause about $\pm 35\%$ uncertainty in the wing bending material weight.

Besides quantifying the magnitude of the uncertainty, the fuzzy set analysis may also allow a designer to select designs with similar performance on the basis of their level of uncertainty. In order to illustrate that point we sought to measure the variation in level of uncertainty of designs with similar weights.

A nominal value for the weight, W_{bn} , was selected as 50000 lbs., which is typical of the weights found in previous HSCT design studies. Then an optimization problem was formulated by employing upper and lower bounds of weight, W_{bu} and W_{bl} , respectively to find two candidate design points with maximal difference in uncertainty bounds ($W_{bu} - W_{bl}$) as

$$\begin{aligned} & \max |(W_{bu} - W_{bl})_2 - (W_{bu} - W_{bl})_1| \\ & |(W_{bn})_1 - 50000| \leq 2500 \\ & |(W_{bn})_2 - 50000| \leq 2500 \end{aligned} \quad (19)$$

There are 10 design variables for this optimization problem: the first five define the configuration variables for point 1 and the remaining five for point 2.

In order to perform the optimization (Eq. 19), two cubic response surfaces were constructed for W_{bu} and W_{bl} based on 314 points selected in the feasible design space. Each point required the use of vertex method, but because the original response surface for the bending material weight was used, the computational cost was not high. The Solver tool of Microsoft EXCEL was used to solve the optimization problem given in Eq. 19. A number of solutions by EXCEL Solver from different initial values defining two design points were obtained. The solutions identified four design points as candidate vertex points, and three of them denoted as Ω_1, Ω_2 and Ω_3 were selected to define a plane.

$$\Omega = \mathbf{a}_1 \Omega_1 + \mathbf{a}_2 \Omega_2 + \mathbf{a}_3 \Omega_3 \quad (20)$$

where $\sum \mathbf{a}_i = 1$ and $0 \leq \mathbf{a}_i \leq 1$ for $i=1, 2, 3$

Equation 20 was used to obtain 66 design points distributed on the alpha plane for which the wing bending material weight and their uncertainty band widths were calculated by the vertex method. Figures 12.a and 12.b show the contour plots over the alpha plane for nominal wing bending material weight and uncertainty band width, respectively. It is seen that for designs with weight of about 50000 lbs. the level of weight uncertainty band can vary from 23000 lbs. to 39000 lbs. In other words, for the designs of the alpha plane similar in terms of wing bending material weight uncertainty may vary from approximately $\pm 23\%$ to approximately $\pm 39\%$. In addition, as a measure of the sensitivity to uncertainty the two alpha plane contour plots together indicate that the uncertainty varies both across and along the isolines of wing bending material.

Concluding Remarks

Response surface approximations for wing bending material weight for five HSCT configuration variables were constructed from finite element analysis based structural optimization results. Improvements in accuracy of approximations were obtained by increasing the number of data points, determining and

repairing outliers, and increasing the order from quadratic to cubic. The largest improvements were achieved through outliers repair by re-optimization. The modeling error and error due to numerical noise were compared along a design line and found that they are of similar magnitude.

In order to avoid additional structural optimizations required for higher order models, the use of a correction response surface was also studied. Correction was performed based on the wing weight equations taken from the FLOPS program. Correction response surfaces allowed lower error levels with quadratic models and smaller number of points.

The uncertainty in the wing bending material weight was studied through fuzzy set theory. The variations in the uncertainty in the design space were illustrated by studying a plane where the bending material weight is nearly constant. Contour plots in that plane indicate that the uncertainty varies by as much as 75% both across and along the isolines of wing bending material. This kind of information may allow a designer to choose between designs having similar wing bending material weight.

Acknowledgment

This work has been supported by NASA grant NAG1-2000.

References

1. Torenbeek, E., "Development and Application of a Comprehensive, Design-sensitive Weight Prediction Method for Wing Structures of Transport Category Aircraft", Delft University of Technology, September 1992, Report LR-693.
2. Balabanov, V., Haftka, R. T., Grossman, B., Mason, W. H., and Watson, L. T., "Multifidelity Response Surface Model for HSCT Wing Bending Material Weight", *ISSMO/NASA/AIAA First Internet Conference on Approximations and Fast Reanalysis in Engineering Optimization*, June 14-27, 1998.
3. Giunta, A. A., Dudley, J. M., Narducci, R., Grossman, B., Haftka, R. T., Mason, W. H., and Watson, L. T., "Noisy Aerodynamic Response and Smooth Approximations in HSCT Design," Proceedings of the 5th AIAA/NASA/ISSMO Multidisciplinary Analysis and Optimization Symposium, Panama City, Florida, September 7-9, 1994, Paper no. 94-4376, pp. 1117-1128.
4. Venter, G., and Haftka, R. T., "Using Response Surface Methodology in Fuzzy Set Based Design Optimization," Proceedings of the 39th

- AIAA/ASME/ASCE/AHS/ASC Structures, Structural Dynamics, and Materials Conference, Long Beach, California, April 20 - 23, 1998, Paper No. 98-1776.
5. Venter, G., and Haftka, R. T., "Response Surface Approximations for Cost Optimization of Dropped Ply Composite Laminates with Uncertainty", AIAA -98-4856.
6. Dong, W., and Shah, H. C., "Vertex Method for Computing Functions of Fuzzy Variables," *Fuzzy Sets and Systems* 24 (1987) 65 -78, North Holland.
7. Myers, R. H., and Montgomery, D. C., *Response Surface Methodology: Process and Product Optimization Using Designed Experiments*. New York: John Wiley & Sons, Inc. 1995.
8. Zadeh, L. A., "Fuzzy Sets," *Information and Control*. Vol. 8, 1965, New York: Academic Press, pp. 29-44.
9. Klir, G., and Yuan, B., *Fuzzy Sets and Fuzzy Logic: Theory and Applications*. USA: Prentice-Hall Inc. 1995.
10. Giunta, A. A., Balabanov, V., Burgee, S., Grossman, B., Haftka, R. T., Mason, W. H., and Watson, L. T., "Variable-Complexity Multidisciplinary Design Optimization Using Parallel Computers", *Computational Mechanics'95 - Theory and Applications*, pp.489-494, 1995. Editors: Alturi, S. N., Yagawa, G., Cruse, T. A., Springer, Berlin.
11. Kaufman, M., Balabanov, V., Burgee, S. L., Giunta, A. A., Grossman, B., Haftka, R. T., Mason, W. H., and Watson, L. T., "Variable-Complexity Response Surface Approximations for Wing Structural Weight in HSCT Design", *Computational Mechanics*, 18(2), pp. 112-126, 1996.
12. Knill, D. L., Giunta, A. A., Baker, C. A., Grossman, B., Mason, W. H., Haftka, R. T., and Watson, L. T., "Multidisciplinary HSCT Design using Response Surface Approximations of Supersonic Euler Aerodynamics", AIAA 98-0905, *36th Aerospace Sciences Meeting and Exhibit*, Reno, NV, January 1998.
13. VMA Engineering, 1767 S. 8th Street, Suite M-200, Colorado Springs, CO 80906, GENESIS User Manual, Version 4.0, October 1997.
14. SAS Institute Inc., SAS Campus Drive Cary, NC 27513, JMP Statistics and Graphics, and User's Guides, Version 3, January 1998.
15. McCullers, L. A., *Flight Optimization System Release 5.92*, NASA Langley Research Center, 1997.

Table 1: Configuration design variables for HSCT with corresponding value ranges

Design Variable	Value
Planform Variables	
Root chord, c_{root}	150 – 190 ft
Tip chord, c_{tip}	7 – 13 ft
Wing semi-span, $b/2$	74 ft
Length of inboard LE, s_{ILE}	132 ft
Inboard LE sweep, L_{ILE}	67° - 76°
Outboard LE sweep, L_{OLE}	25°
Length of inboard TE, s_{ITE}	Straight TE
Inboard TE sweep, L_{ITE}	Straight TE
Airfoil Variables	
Location of max. thickness, $(x/c)_{max-t}$	40%
LE radius, R_{LE}	2.5
Thickness to chord ratio at root, $(t/c)_{root}$	1.5 – 2.7%
Thickness to chord ratio LE break, $(t/c)_{break}$	$(t/c)_{break}=(t/c)_{root}$
Thickness to chord ratio at tip, $(t/c)_{tip}$	$(t/c)_{tip}=(t/c)_{root}$
Fuselage Variables	
Fuselage restraint 1 location, x_{fus1}	50 ft
Fuselage restraint 1 radius, r_{fus1}	5.2 ft
Fuselage restraint 2 location, x_{fus2}	100 ft
Fuselage restraint 2 radius, r_{fus2}	5.7 ft
Fuselage restraint 3 location, x_{fus3}	200 ft
Fuselage restraint 3 radius, r_{fus3}	5.9 ft
Fuselage restraint 4 location, x_{fus4}	250 ft
Fuselage restraint 4 radius, r_{fus4}	5.5 ft
Nacelle, Mission, and Empennage Variables	
Inboard nacelle location, $y_{nacelle}$	20 ft
Distance between nacelles, $D_{nacelle}$	6 ft
Fuel weight, W_{fuel}	280000 – 350000 lb.
Starting cruise altitude	65000 ft
Cruise climb rate	100 ft/min
Vertical tail area	548 ft ²
Horizontal tail area	No horizontal tail
Engine thrust	39000 lb.

Table 2: Load cases in HSCT design study

Load Case	Mach Number	Load Factor	Altitude (ft.)
High-speed cruise	2.4	1.0	63175
Transonic climb	1.2	1.0	29670
Low-speed pull-up	0.6	2.5	10000
High-speed pull-up	2.4	2.5	56949
Taxiing	0.0	1.5	0

Table 3: RMS Error estimator (RMSE) for response surface approximations on wing bending material weight

RS	RMSE (lb.)	% of average WBMW	R _a ²
43 points, full quadratic model	5460.9	9.9	0.9659
43 points, reduced quadratic model	4976.7	9.0	0.9717
70 points, full quadratic model	4709.6	8.7	0.9668
70 points, quad. and 6 cubic terms model	4652.9	8.6	0.9676
112 points, full quadratic model	4592.3	8.6	0.9520
43 repaired points, full quadratic model	4193.5	7.7	0.9794
112 repaired points, quadratic model	3396.6	6.5	0.9800
112 repaired points, reduced cubic model (39 terms)	2179.9	4.2	0.9918

Table 4: Variations of optimization results on different computers

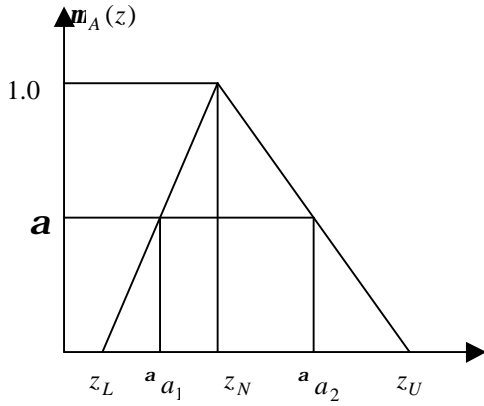
Configuration	Wing Bending Material Weight (lb.)		
	Large move limits on PC	Small move limits on PC	Large move limits on Unix
1	66080	86106	74714
2	70370	102077	90128
7	60286	64139	56808
9	78054	67447	81950

Table 5: Errors for correction response surface approximations for wing bending material weight

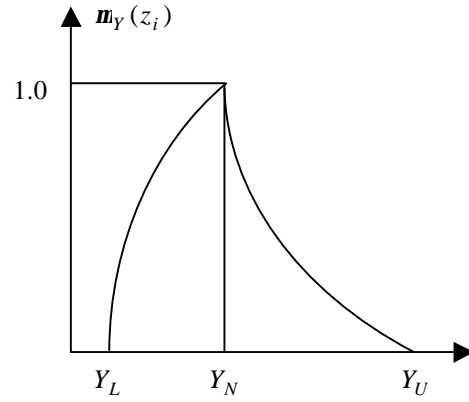
RS	RMSE (lb.)	% of average WBMW	R _a ²
43 points, full quadratic model	3413.5	6.2	0.9735
43 points, reduced quadratic model	2769.1	5.0	0.9738
70 points, full quadratic model	3640.5	6.8	0.9606
112 points, full quadratic model	4126.7	7.8	0.9440
112 points, reduced quadratic model	3923.6	7.4	0.9499
43 repaired points, full quadratic model	2409.7	4.4	0.9864
43 repaired points, reduced quadratic model	2182.8	4.0	0.9888
112 repaired points, quadratic model	2886.3	5.5	0.9713
112 repaired points, reduced quadratic model	2824.6	5.4	0.9725
112 repaired points, reduced cubic model (37 terms)	2332.7	4.4	0.9812

Table 6: Uncertainty levels and ranges for fuzzy variables

Fuzzy Variable	Uncertainty	Variable Range	
		minimum	maximum
x ₁ , Root chord length (ft)	± 2%	153.1	186.3
x ₂ , Tip chord length (ft)	± 5%	7.37	12.38
x ₃ , L.E. sweep angle (degree)	± 1.5%	68.0	74.9
x ₄ , t/c	± 3%	0.0155	0.0260
x ₅ , Fuel weight (lbs.)	± 10%	311111	318182
ρ, Density (lb/ft ³)	± 5%	281.7	
s _y , Yield stress (lb/ft ²)	- 5% and +15%	1.32 x 10 ⁷	



(a) Triangular membership function of a fuzzy set **A**



(b) Membership function of a fuzzy function **Y**

Figure 1: Membership functions

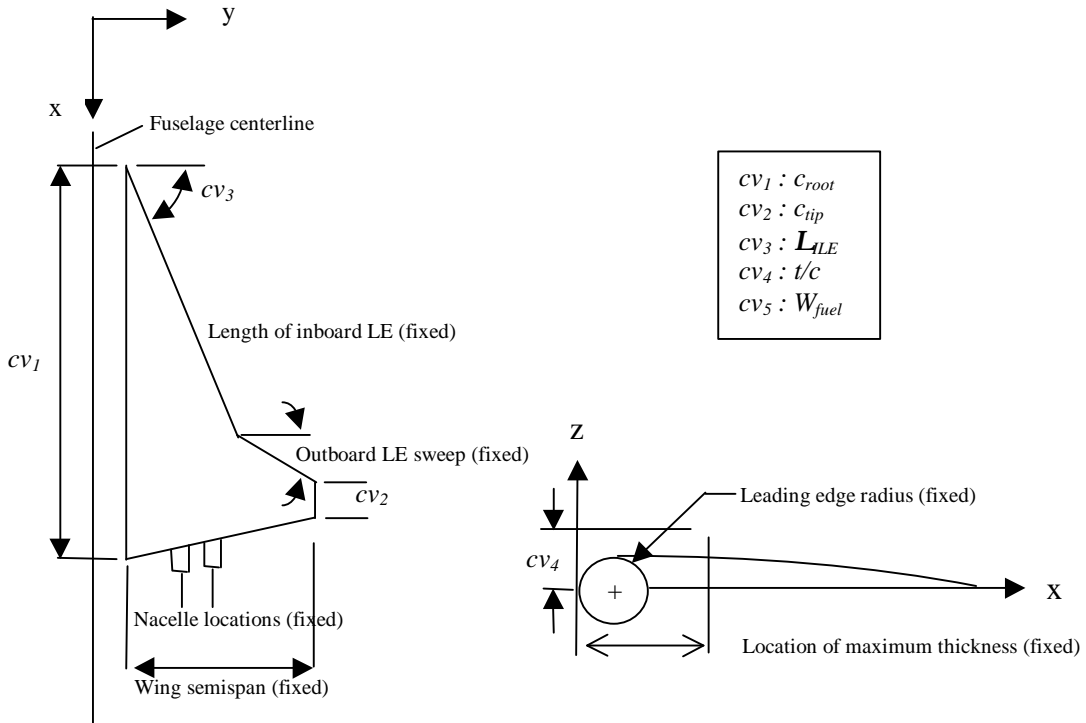


Figure 2: HSCT wing planform and 5 configuration variables

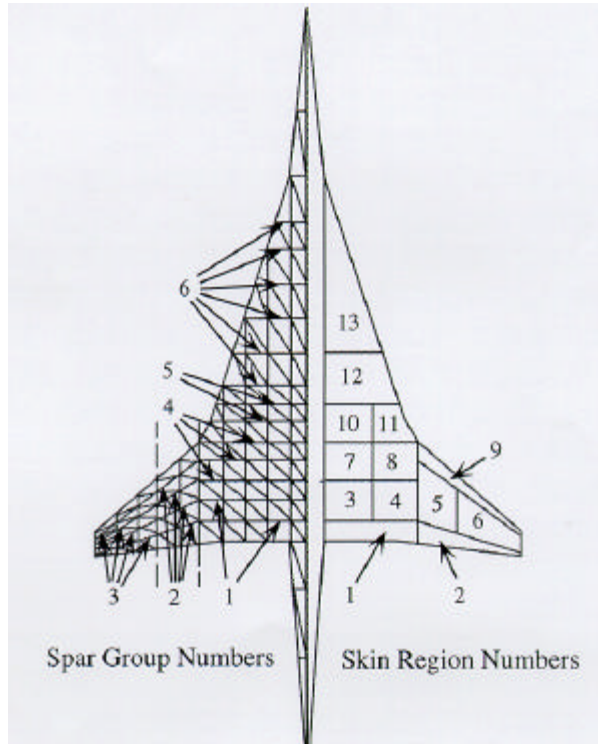


Figure 3: HSCT finite element model and structural design variables

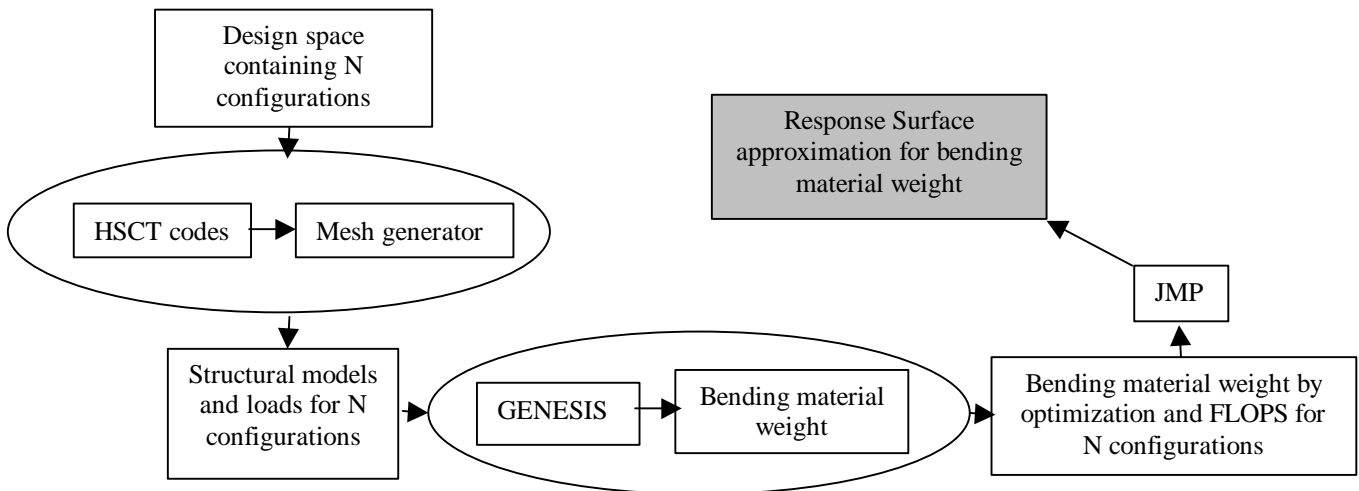
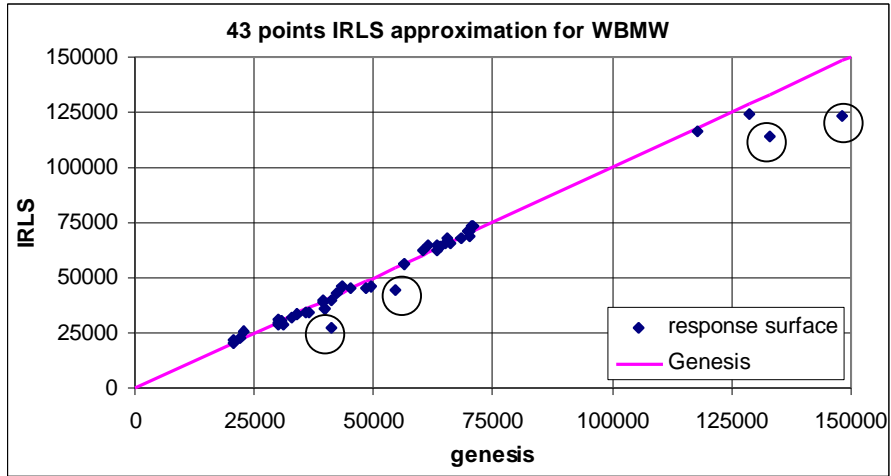
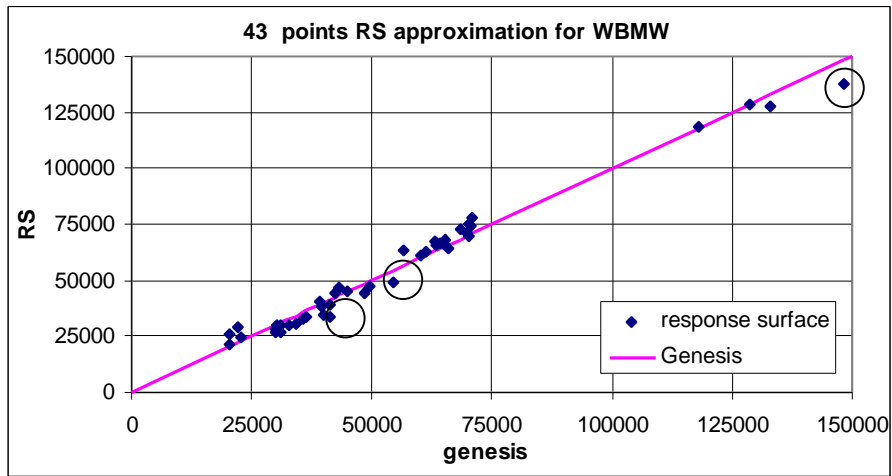


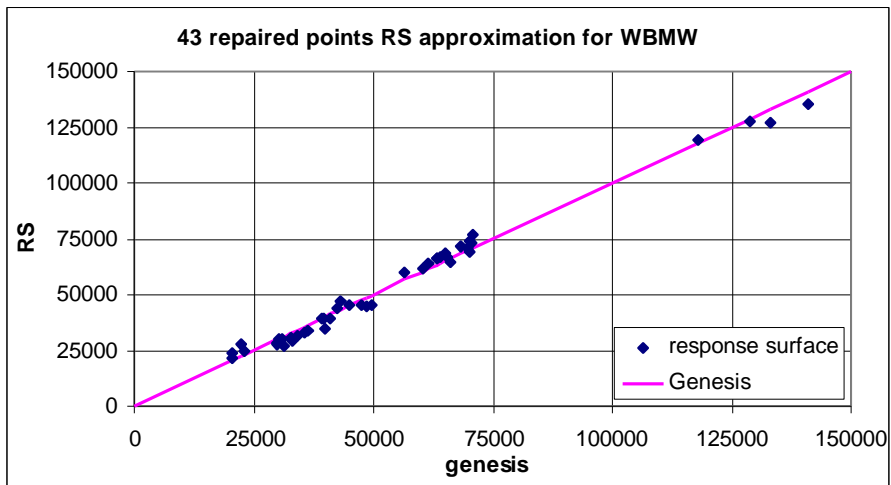
Figure 4: Flow chart for RS approximation procedure



(a) IRLS approximation and detected outliers

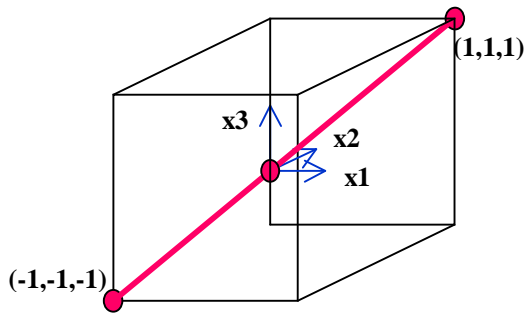


(b) RS approximation for original data (points that were successfully repaired are circled)



(c) RS approximation for repaired data

Figure 5: Response surface outliers and effect of repair



variable	1	2	3	19	20	21	
1	-1.0	-0.9	-0.8	0.8	0.9	1.0
2	-1.0	-0.9	-0.8	0.8	0.9	1.0
3	-1.0	-0.9	-0.8	0.8	0.9	1.0
4	-1.0	-0.9	-0.8	0.8	0.9	1.0
5	-1.0	-0.9	-0.8	0.8	0.9	1.0

(a) Design line for 3-D design box

(b) Design line for five configuration variables

Figure 6: Extreme value design line in a design space

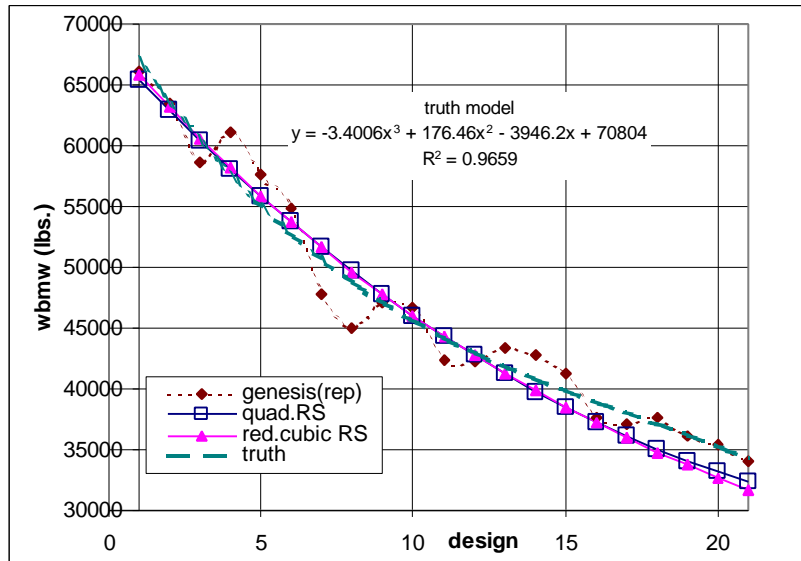


Figure 7: Comparison of RS approximations and GENESIS results along extreme value design line

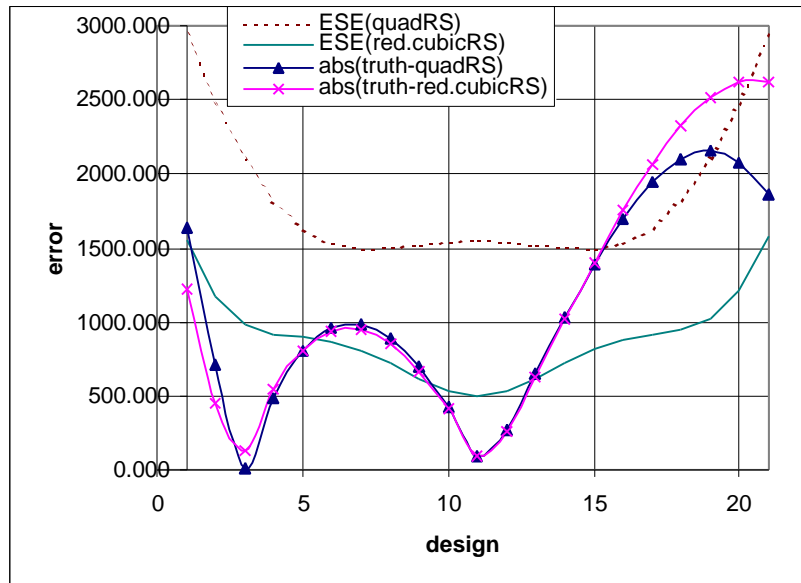


Figure 8: Estimated Standard Error (ESE) and absolute errors based on truth model for RS approximations

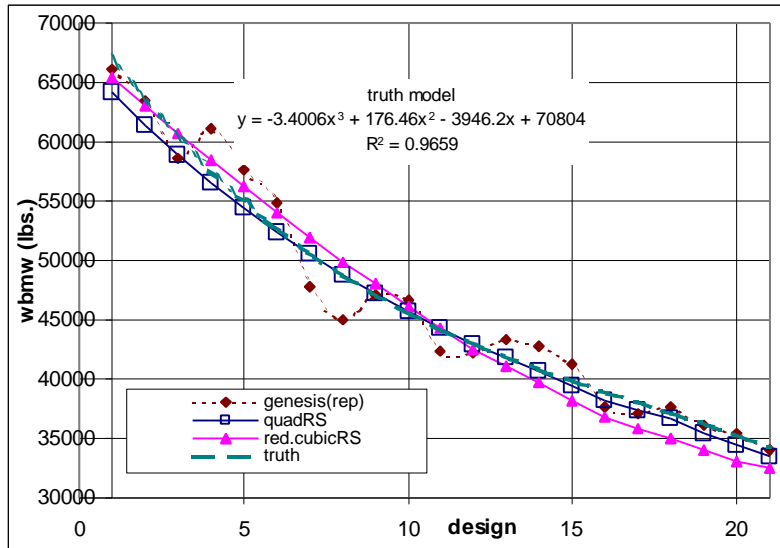


Figure 9: Comparison of correction RS approximations and GENESIS results along extreme value design line

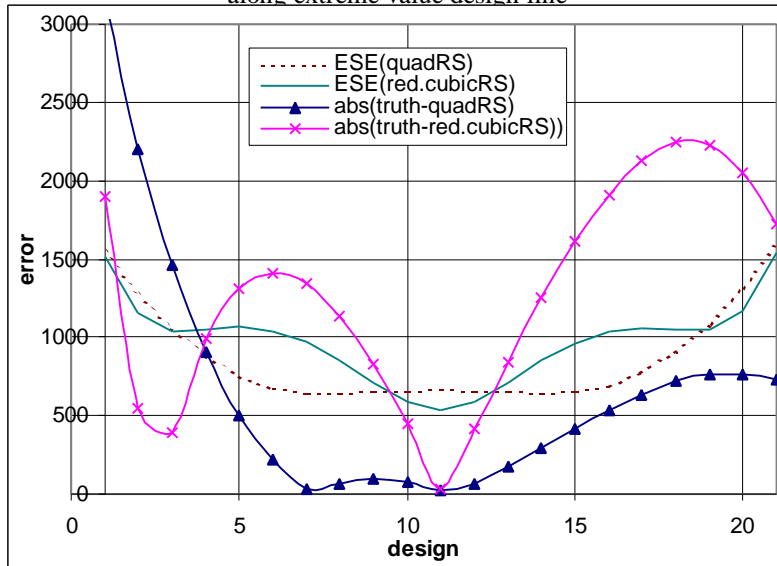


Figure 10: Estimated Standard Error (ESE) and absolute errors based on truth model for correction RS approximations

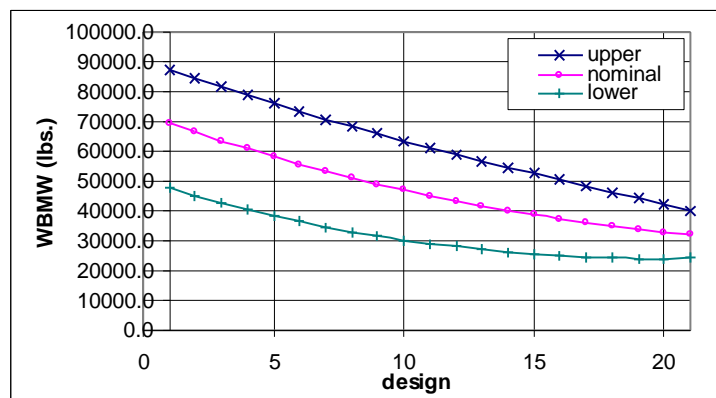
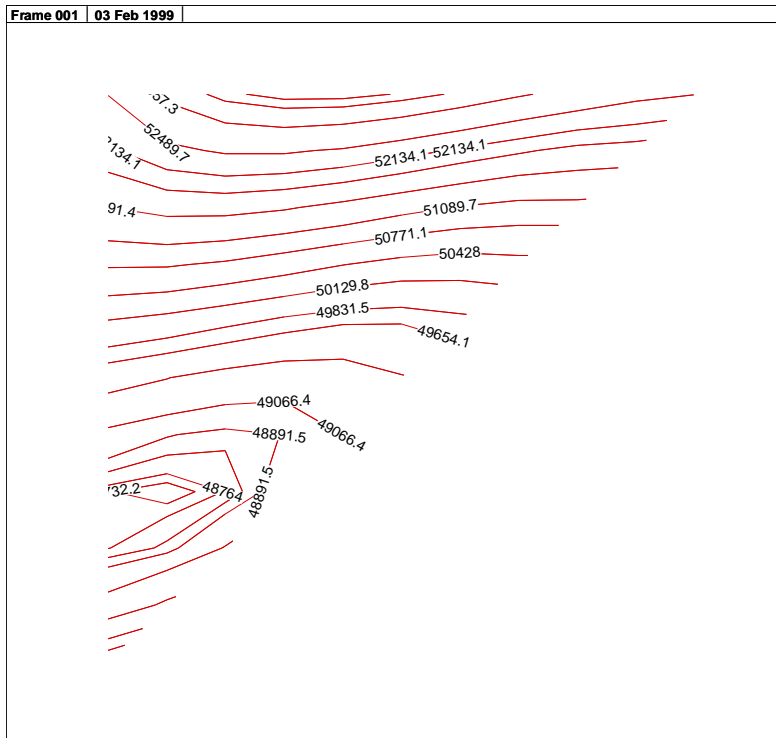
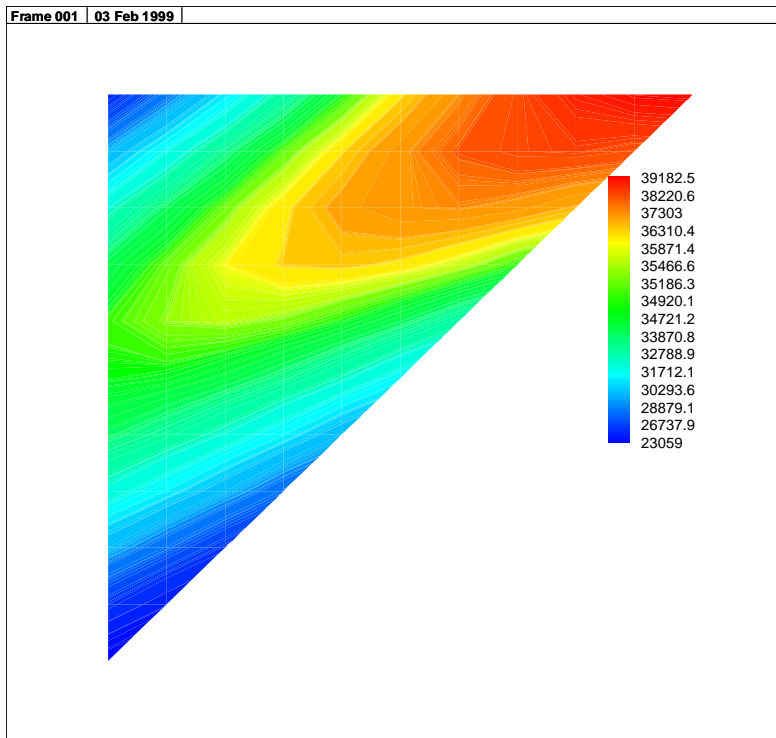


Figure 11: Uncertainty in WBMW along extreme value design line



(a) Nominal wing bending material weight contours



(b) Uncertainty band width (upper bound minus lower bound) contours

Figure 12: Contours in plane with almost constant wing bending material weight